Solid Freeform Fabrication 2024: Proceedings of the 35th Annual International
Solid Freeform Fabrication Symposium – An Additive Manufacturing Conference
Reviewed Paper

REDUCTION OF AGING MECHANISMS IN A POLYAMIDE 66 MATERIAL FOR USE IN THE LASER-BASED POWDER BED FUSION PROCESS

J. Hofmann*, A. Wegner†, K. Wudy*

*Technical University of Munich, TUM School of Engineering and Design, Professorship of Laser-based Additive Manufacturing, Freisinger Landstraße 52, 85748 Garching, Germany
†AM POLYMERS GmbH, Hanns-Martin-Schleyer-Straße 9e, 47877 Willich, Germany

Abstract

In laser-based powder bed fusion, aging mechanisms caused by prolonged thermal exposure affect polymers. Therefore, new material is blended with used powder to maintain acceptable component properties and save costs. However, this method is limited for high-performance plastics with high processing temperatures (> 200 °C), like polyetheretherketone (PEEK). Filled polyamide 66 (PA66) compounds with lower processing temperatures, lower service temperatures but comparable mechanical properties represent a promising alternative for aerospace and automotive components. However, PA66 cannot be reliably processed and reused so far due to the degradation of the material properties during processing. Therefore, this study examines processed and artificially aged PA66 powder using a vacuum-drying oven to understand the aging mechanisms during processing. An analysis of the thermal and rheological properties of neat PA66 and filled compounds revealed significantly decreased aging effects at lower storage temperatures and oxygen levels. Furthermore, a novel filled and modified PA66 compound was investigated, balancing thermo-oxidation and post-condensation effects while maintaining high mechanical properties (tensile strength > 70 MPa) when using 50 % recycled material.

Introduction

In laser-based powder bed fusion of plastics (PBF-LB/P), components are produced by successive melting of polymeric powder applied in layers using a laser. The powder is heated close to the onset of melting. Following laser exposure, the melted material decays to processing temperature and remains liquid. This phenomenon is caused by temperature- and time-dependent hysteresis between crystallization and melting. Since the component remains liquid at the same temperature as the unmelted powder material, no additional support structures are required, which is the reason for the high design freedom in PBF-LB/P. However, the unused powder cannot be reused in subsequent processes, as material properties deteriorate due to the prolonged thermal stress at temperatures close to the melting point. [1]. For polyamide 12 (PA12), the material's rheological [2], thermal [1], and powder bulk properties [3] change since material aging alters the molecular structure with increasing storage temperature and time. These changes affect the fusion of particles, resulting in reduced mechanical properties [3]. Therefore, it is a common practice in the industry to blend the used powder with 30 to 50 wt% of virgin powder for PA12 [2].

In addition to PA12, other semi-crystalline materials are commercially available, including polypropylene (PP), polyamide 6 (PA6), polyethylene (PE), and thermoplastic polyurethane (TPU) [4]. These engineering plastics are processed below 250 °C and can be reused in subsequent build processes when blended with virgin powder. In contrast, the processing and reuse of high-performance plastics is more challenging. These include polymers such as polyphenylene sulfide (PPS) and the polyaryletherketone (PAEK) family, which includes polyetheretherketone (PEEK) and polyetherketoneketone (PEKK), which differ only in the ratio of ether to ketone linkages. For example, the reuse of the polymer powders with the trade names "EOS PEEK HP3" (processed at 368 °C) [5] and "Toraymill PPS-GF 25" (processed at 280 °C) [6] is not possible without a significant reduction in the component properties.

On the other hand, filled polyamide 66 (PA66) compounds, when injection molded, exhibit mechanical properties nearly comparable to the aforementioned high-performance plastics [7]. While its service temperature is lower, filled PA66 can be processed in PBF-LB/P at a more manageable temperature (250°C). Nevertheless, it is currently impossible to reuse PA66 in PBF-LB/P either. This is due to a lack of understanding of the aging mechanisms when PA66 is processed in PBF-LB/P.

Aging mechanisms of polyamide 66

Aging mechanisms can be classified into two main categories: physical and chemical. Physical aging, such as post-crystallization and relaxation, involves reversible changes in the arrangement of polymer chains [8]. In contrast, chemical aging mechanisms result in permanent changes to the polymer chains, such as chain scission, branching, and crosslinking [8]. In the case of polyamides, chemical aging mechanisms, including thermo-oxidation, hydrolysis, and post-condensation, are predominantly attributed to the influence of heat, oxygen, and moisture [8]. These mechanisms change the molecular weight and, thus, affect the material properties relevant to PBF-LB/P processing [9].

The thermo-oxidation of polyamides has been extensively studied for temperatures ranging from 90 to 180°C. In the presence of oxygen, the degradation rate generally increases with temperature, as evidenced by the Arrhenius law, which governs the thermo-oxidation kinetics of aliphatic polyamides [10]. However, the type and extent of molecular changes depend on the storage conditions and duration. In general, thermo-oxidation is a complex free radical chain mechanism encompassing three stages: initiation, propagation, and termination [10]. Given high temperatures and an oxygen-rich atmosphere, thermo-oxidation leads to an increase in carboxyl groups and a decrease in amino groups, which is accompanied by a release of volatile components such as carbon dioxide [11], ammonia [11], and others [12]. The number and ratio of amino and carboxyl end groups significantly influence the rate of thermo-oxidative degradation [13]. Furthermore, in semi-crystalline polymers, oxygen diffusion predominantly occurs in amorphous regions, leading to their preferential oxidation before the crystalline regions are attacked [14]. Consequently, the rate of thermo-oxidation decreases with increasing crystallinity [14]. In addition, PA66 experiences recrystallization at elevated temperatures, a physical aging mechanism that affects the degree of crystallinity [15]. In conclusion, low residual oxygen content in the processing chamber is essential for limiting material aging of PA66 in PBF-LB/P.

Moreover, polyamides and other polycondensates undergo solid-state post-condensation between their glass transition temperature and the melting point since no chain termination or transmission occurs in condensation reactions [16]. Consequently, the chain ends remain reactive after polymerization [16]. If PA66 is subjected to high temperatures, polyamide chains' amine and carboxyl end groups react and form amide bonds [15]. This solid-state post-condensation process promotes chain extension and increases the molecular weight [15]. The rate constant of post-condensation is influenced by several factors, including temperature, end group concentration, particle size, inert gas flow rate, and degree of crystallinity [17].

Furthermore, the oxidation of polyamides is subject to diffusion limitations, which restrict the oxidation process to a thin layer in which the molar mass is significantly reduced [18]. This phenomenon arises from the faster consumption of oxygen in oxidation reactions at the surface compared to its diffusion into the material [19]. The degraded surface impedes oxygen diffusion and thus reduces further thermo-oxidation in the core [14]. Nevertheless, as other chemical aging mechanisms, such as post-condensation, are still present, the molar mass typically increases in the core [8]. Consequently, the surface layer acts as a barrier for oxygen from the outside and gaseous degradation products from the inside [20]. In PA6, studies between 120 and 180 °C have demonstrated that oxygen diffusion limitation, described by Fick's Law, results in parabolic oxidation profiles [21]. These oxidation profiles develop from the sample surface towards the core [21]. In injection molding, antioxidants are often added to PA66 to reduce the thermo-oxidation reaction rate, leading to a less pronounced oxidation profile between the surface layer and the core [14]. In addition, increasing the temperature increases oxidation but reduces the thickness of the oxidized layer [22]. For PA66, oxidized layer thicknesses of 0.2 to 0.6 mm have been observed at 110 to 130°C [22]. This has considerable implications for PA66 powder in PBF-LB/P as particle sizes of industrial powders range from 10 to 120 µm in diameter [4].

The maximum moisture content of PA66 is reported to be up to 3.8 % if stored in a standard climate [8], which is attributed to the high hydrophilicity of amide bonds [23]. Furthermore, it should be noted that the maximum moisture content of PA66 depends on the degree of crystallization, as water is absorbed in the amorphous phase [24]. The absorbed water acts as a plasticizer in PA66, leading to reversible and irreversible changes in the material's properties [25]. Reversible changes include alterations in thermal and mechanical properties resulting from increased chain mobility [25], while irreversible damage can occur through hydrolysis, a chain scission reaction involving amide groups and water [26]. Hydrolysis proceeds simultaneously with condensation, where amino and carboxyl end groups of longer chains combine to form new amide bonds [26]. This concurrent process results in a temperature-dependent plateau in viscosity and molecular weight [27]. Additionally, the oxygen diffusion coefficient of PA66 increases with moisture content due to enhanced chain mobility [28]. This elevated oxygen diffusion promotes thermo-oxidation [12]. Consequently, effective drying is crucial to prevent hydrolysis of PA66 in PBF-LB/P.

In conclusion, the changes in molecular weight and the resulting changes in component and material properties over the aging period result from the relationship between the aforementioned aging mechanisms [29]. Additionally, crosslinking and branching are reported during the thermal degradation of PA66 [15]. These reactions can occur through complex reactions involving radicals formed during chain scission or caused by additives that influence the degradation pathways [15]. However, these events are relatively rare compared to chain scission (thermo-oxidation and hydrolysis) and chain extension (post-condensation), especially for polyamide processing in PBF-LB/P [1]. Similarly, other aging mechanisms, such as photo-oxidative aging [8] or mediainduced aging [8], are likely to play a minor role in PBF-LB/P. In addition to these chemical and physical aging mechanisms, the thermal decomposition of PA66 can also lead to significant changes in the molecular structure and the release of volatile components above 275°C [30]. However, the PA66 powder is processed at around 250 °C. Given that a short-term temperature increase of 25 to 75 K is anticipated during laser exposures [31], it can be reasonably assumed that thermal decomposition will have a negligible impact on PA66 processing in PBF-LB/P.

An extensive review of the oxidative and non-oxidative aging of polyamide 66 can be found in [15] and [30], respectively. However, as demonstrated, most research on the aging of PA66 focuses on two areas: long-term heat exposure below 200°C (up to 10,000 h), which reflects real-world conditions for components, and short-term heat exposure above 275°C (up to 2 h), which mimics the high temperatures encountered during processes like injection molding and extrusion. In contrast, the aging behavior of PA66 under PBF-LB/P processing conditions, particularly storage at 250 °C for 0 to 48 hours in a nitrogen atmosphere with up to 2 % residual oxygen, has not been studied yet. This is a critical issue given the use of powder particles in PBF-LB/P, which leads to a high specific surface area, potentially accelerating aging. Fig. 1 visualizes the influences on the different aging mechanisms in PA66 as well as their interactions and impact on material properties. The interdependencies between these aging mechanisms make it difficult to predict the effect of aging on material properties. When changes in relevant properties such as viscosity or melting temperature are significant, it is essential to modify processing parameters to produce dense parts with sufficient mechanical properties. However, in the case of neat PA66, these changes are so severe that it is not possible to process it reliably in PBF-LB/P.

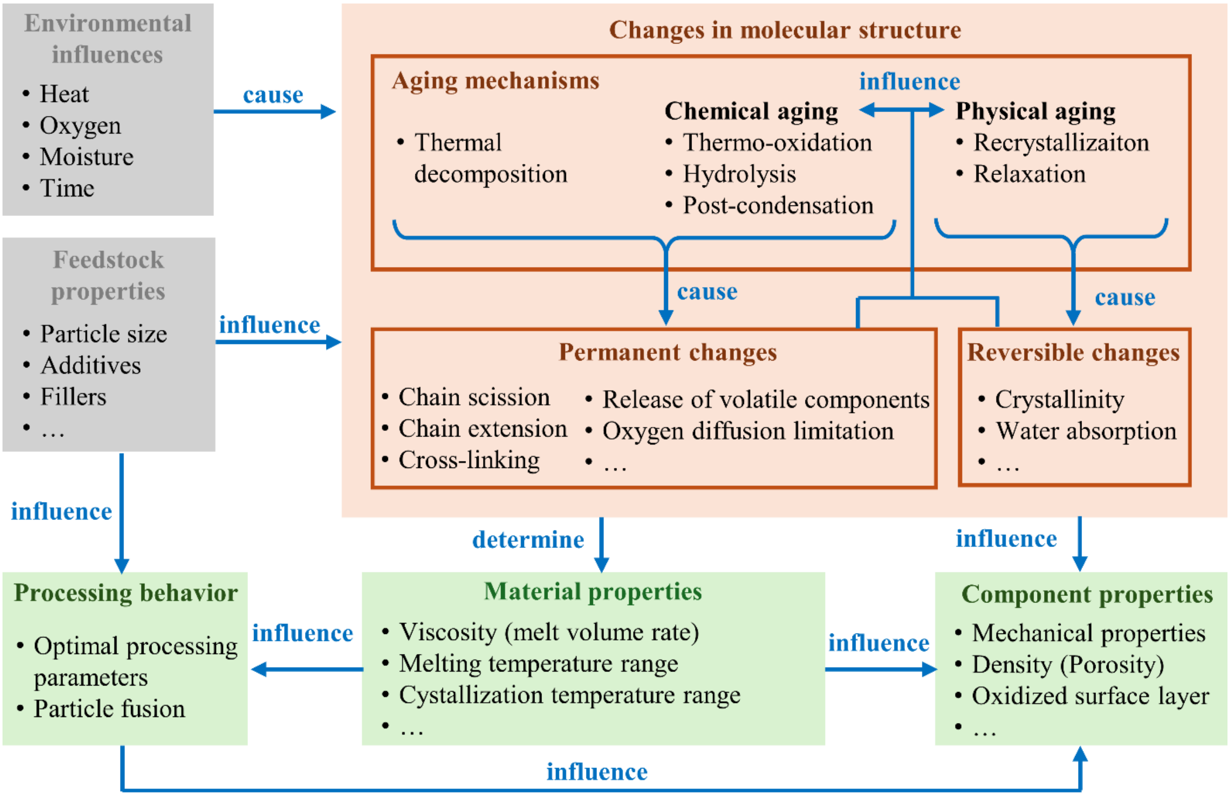

Figure 1: Relevant influences of the aging mechanisms occurring during the processing of polyamides in PBF-LB/P and their interactions

Therefore, this study examines the impact of PA66 aging in PBF-LB/P on the thermal and rheological properties of the powder and material. This is particularly important for the recycling of unused powder in subsequent processes.

Methodology

2.1 Materials

To date, no PA66 material can be processed in a reliable and reproducible manner using PBF-LB/P. This is attributed to the degradation of the material properties of PA66 powder when subjected to processing temperatures of approximately 250 °C. This research investigates how different processing conditions affect the thermal and rheological properties of neat PA66 powder in the PBF-B/P process, which is crucial for understanding how to improve its processability. At first, experiments are conducted in a vacuum oven to determine the influence of different processing temperatures and oxygen contents, as the powder cannot be processed. In addition to the neat PA66, a modified PA66 powder (Rolaserit® PA66-CP08, AM Polymers) is also under investigation. While the exact formulation of this modified PA66-CP08 powder is unknown, this research aims to determine whether it can maintain consistent properties during thermal storage. This is key for ensuring the material can be reused in subsequent processes. To this end, melt flow indexing (melt volume rate, MVR) and differential scanning calorimetry (DSC) will be employed.

Once a suitable processing temperature range has been identified, the Rolaserit® PA66-CP08 powder is fabricated into tensile test specimens and density cubes to examine the part density and mechanical properties. Additionally, two carbon-fiber-filled PA66 powders (Rolaserit® PA66-CP08-CF and PA66-CP08-CF04, AM Polymers) are studied to assess if adding fillers can further enhance the material's mechanical properties. The exact ratio and type of fillers in these powders are also unknown. A parameter study is performed to determine the extent to which laser and scan parameters affect the resulting part properties. All powder variants are processed in virgin condition, while Rolaserit® PA66-CP08 and PA66-CP08-CF04 are also processed as a 1:1 blend of virgin and used powder. This will demonstrate whether the materials can retain their high mechanical properties when the powder is reused in subsequent processes. In addition to tensile testing, the heat deflection temperature (HDT) is determined to evaluate the performance of components in high-temperature environments. In conclusion, this study examines four distinct development grades of Rolaserit® PA66 (AM Polymers). Table 1 summarizes the different variations in powder composition and the respective experiments conducted with each powder.

Table 1: Overview of the composition of the PA66 powders used

Name	Modified	Filled	Powder characterization	Oven storage & material characterization	Build process & part characterization
Rolaserit® PA66	No	No	Bulk density, Particle size	MVR, DSC	-
Rolaserit® PA66-CP08	Yes	No	Bulk density, Particle size	MVR, DSC	Tensile testing, HDT
Rolaserit® PA66-CP08-CF	Yes	Yes	Bulk density, Particle size	-	Tensile testing, HDT
Rolaserit® PA66-CP08-CF04	Yes	Yes	Bulk density, Particle size	-	Tensile testing

2.2 Thermal aging of the powder samples

Different environmental conditions may affect process-relevant material properties when polyamide powder is stored in an oven. For instance, PA66 is reported to undergo thermal degradation at 90 °C when stored in an oxygen-rich atmosphere, such as ambient air [10]. However, the thermo-oxidation is expected to be minimal if the polyamides are stored under vacuum or in a nitrogen atmosphere [9]. Therefore, all powders are first dried in a vacuum oven (80 °C for 24 h at 0.1 mbar) to remove excess moisture and ensure consistent powder conditioning before oven storage. This powder serves as a reference (0 h) in the subsequent rheological and thermal properties analysis.

Following powder conditioning, the material is subjected to artificial aging in a vacuum drying oven (VT 6060 P-BL, Thermo Electron LED) in order to reproduce the effects of the printing process over time for the Rolaserit® PA66 base material and the modified Rolaserit® PA66-CP08 variant. In addition, samples are weighed before and after thermal aging to track weight loss and monitor potential material degradation. As illustrated in Table 2, the study focused on the influence of the oven temperature and the oxygen levels. An indirect method was used to set the target oxygen concentration in the chamber without an oxygen sensor. This involved applying a controlled vacuum level to remove a known proportion of the initial air. The chamber was then purged with nitrogen to achieve the desired oxygen concentration.

Table 2: Parameters used for artificial thermal aging in the vacuum drying oven

Storage temperature	250 °C, 230 °C
Oxygen content	0.05 % O_2, 2 % O_2
Storage time	0, 1, 3, 6, 24 h
Powder materials	Rolaserit® PA66 Rolaserit® PA66-CP08

2.3 Powder characterization

2.3.1 Particle size, shape, and bulk properties

The bulk density (DIN EN ISO 60) is determined to characterize the powder flowability. Dynamic image analysis (Camsizer, Microtrac) is conducted (ISO 13322-2) to determine the particle sizes below which 10 %, 50 %, and 90 % of all particles can be found. The particle shape and visual appearance are examined using a digital microscope (VHX-7000, Keyence).

2.3.2 Thermal powder properties

The thermal properties of the powder are determined by differential scanning calorimetry (DSC 300 Caliris, Netzsch). Two heating and cooling cycles (25 to 275 °C with 10 K/min) are performed in a nitrogen atmosphere. The onset, peak, and end of the melting and crystallization temperature range are determined according to DIN EN ISO 11357-3. Three samples are tested for each combination of powder and test condition.

2.3.3 Rheological powder properties

The melt volume rate (MVR) is determined using a melt flow indexer (Mflow, ZwickRoell) according to DIN EN ISO 1133 (275 °C, 2.16 kg). The test is repeated three times with six measuring sections for each powder mixture.

2.4 Processing and part characterization

The PA66 powders are processed on an industrial PBF-LB/P system (ST252P, Farsoon) in a nitrogen atmosphere containing 0.8 % oxygen (integrated O_2 sensor reading). The Laser and scan parameters are detailed in Table 3. For all materials, only the laser power is varied. However, for Rolaserit® PA66-CP08-CF04 an increased outline laser power is used. The surface temperature is set to 248 °C. After processing, all samples are manually sandblasted.

The density of the fabricated cubes (21-27x15x8 mm³) is determined by measuring the dimensions with a caliper gauge and weighing the sampling following DIN EN ISO/ ASTM 52924:2013. In addition, tensile test specimens are fabricated with their long axes oriented in the xy-plane. The tensile test sample design followed the specifications of DIN EN ISO 527, Type 1A (cross-section: 10x4 mm²) for Rolaserit® PA66-CP08 and PA66-CP08-CF. Tensile testing (Z020 M evo, MultiXtense, ZwickRoell) is conducted for as-built (dry) states using a 5 mm/min displacement rate. The design of the Rolaserit® PA66-CP08-CF04 specimens follows DIN EN ISO 527, Type 1BA, with a modified cross-section of 5x4 mm². A DARTO PM 5 tensile tester with a 5 kN load cell and a displacement rate of 5 mm/min is used for these smaller samples. Furthermore, bending beams are produced to measure the heat deflection temperature (HDT). The HDT A and HDT B (ISO 75) are determined (HDT/Vicat A measuring system, ZwickRoell, heating rate: 120 K/min) to assess the temperature at which the sample elongation exceeds 0.2 % under a constant load of 1.8 MPa and 0.45 MPa, respectively.

Table 3: Laser and scan parameters used for the build process

Energy density in J/mm³	Laser power in W	Scan speed in mm/s	Hatch distance in mm	Layer height in mm	Outline laser power in W	Outline scan speed in mm/s
0.24	45	12,700	0.15	0.1	22	3,048
0.26	50	12,700	0.15	0.1	22 (25)	3,048
0.29	55	12,700	0.15	0.1	22 (25)	3,048
0.31	60	12,700	0.15	0.1	22 (25)	3,048
0.34	65	12,700	0.15	0.1	(25)	3,048

Results and Discussion

3.1 Influence of thermal aging on physical powder properties and flowability

A dense powder bed is a prerequisite for dense as-build parts, which are directly influenced by the powder flowability, particle size, and shape [4]. The largest particles determine the layer height for processing, while large portions of small particles can increase adhesive forces between particles, hindering powder flowability [32]. Table 4 shows a D10 in the 17 to 32 µm range, D50 of approx. 60 µm, and D90 around 97 to 114 µm. This is consistent with other industrial polymer powders (10 – 120 µm) [4]. Furthermore, the particle size distribution between Rolaserit® PA66 and the PA66-CP08 remains largely unchanged. In addition, particle shape, characterized by roundness and roughness, affects flowability and packing density [33]. As illustrated in Fig. 2, the powder particles are irregularly shaped with rough surfaces, which suggests they are produced via milling.

The filled Rolaserit® PA66-CP08-CF exhibits a slight increase in bulk density, which is to be expected due to the higher material density (1.26 g/cm³ according to the material data sheet). However, the increase should be much higher, as the material density of the unfilled variants is approximately 1.14 g/cm³. It can be assumed that the carbon fibers in the PA66-CP08-CF and PA66-CP08-CF04, shown in Fig. 2, prevented a stronger compaction during the pouring process.

Table 4: Overview of powder analyses carried out on different Rolaserit® development grades in varying conditions

Polymer	Condition	Bulk density in g/cm³	Particle size		
			D10 in µm	D50 in µm	D90 in µm
Rolaserit® PA66	virgin	0.456 ± 0.006	26.5	66.5	99.7
	1:1 blend (used:virgin)	0.440 ± 0.003	31.8	70.7	99.7
	used 1:1 blend (after processing)	0.430 ± 0.001	31.7	68.2	97.8
Rolaserit® PA66-CP08	virgin	0.447 ± 0.004	25.9	68.0	112.8
	used (after processing)	0.379 ± 0.004	24.9	65.2	113.7
Rolaserit® PA66-CP08-CF	virgin	0.474 ± 0.004	17.0	58.3	98.2
	used (after processing)	0.406 ± 0.005	17.2	56.2	101.1
Rolaserit® PA66-CP08-CF04	virgin	0.460 ± 0.005	17.5	58.7	97.1
	used (after processing)	0.354 ± 0.025	18.1	57.5	101.9
	1:1 blend (used:virgin)	0.463 ± 0.003	18.4	61.3	98.1
	used 1:1 blend (after processing)	0.404 ± 0.004	17.2	55.1	96.6

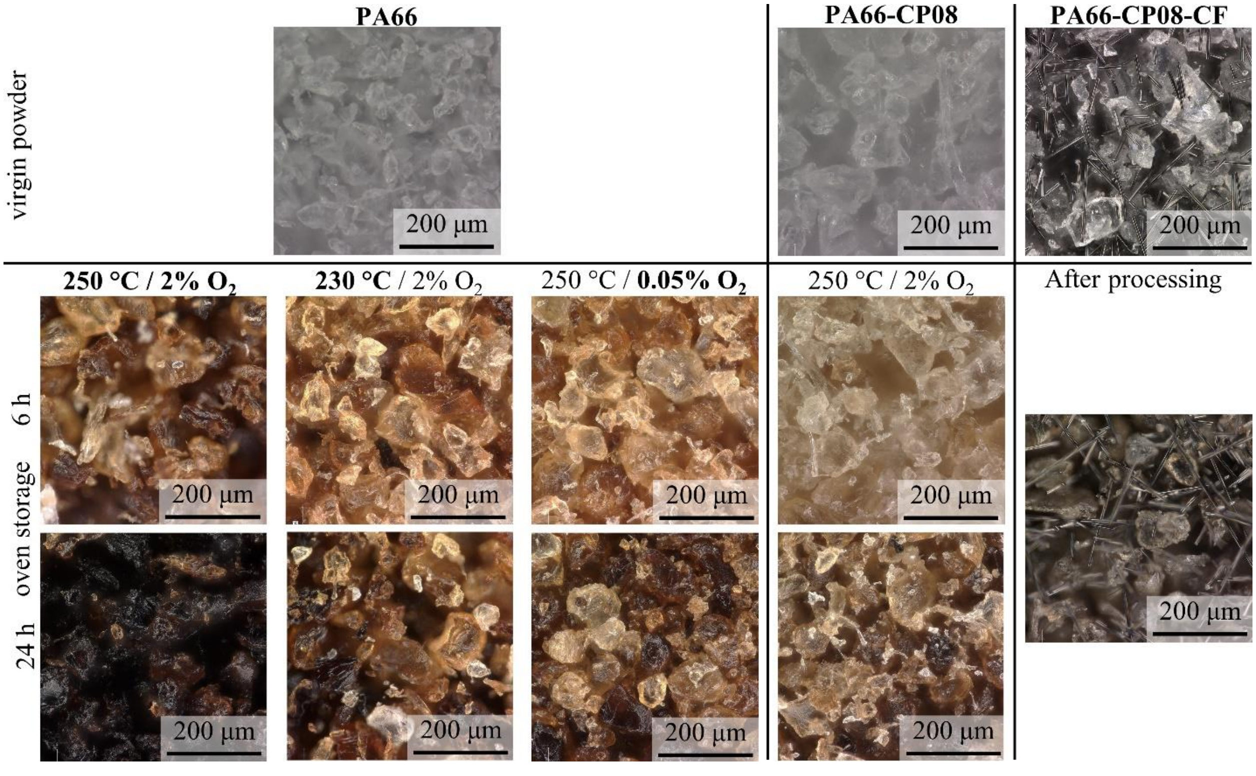

Figure 2: Exemplary microscopy images of the PA66 powders before and after oven storage and processing

After processing, the used powders show a drop in bulk density, indicating a reduction in powder flowability. For unfilled Rolaserit® PA66, the material has no significant change even after recycling (1:1 blend of virgin and used powder). However, for the filled Rolaserit® PA66-CP08-CF04, the decrease in bulk density for the used powder of partly reclaimed powder (1:1 blend of virgin and used powder) is less than for the used powder stemming from virgin powder, indicating that this powder is optimized for reuse. Overall, it can be concluded that bulk density and particle size remain nearly constant even after recycling and reuse. In conclusion, there is no significant deterioration of particle properties and bulk density due to aging or recycling.

In this study, all powders lost 1.6 to 1.9 % of their mass during drying. Upon the subsequent oven storage, Rolaserit® PA66 displays similar weight loss in the first 3 h, regardless of storage conditions (see Fig. 3). Furthermore, oven storage induced yellowing in all samples, with varying intensity (compare Fig. 2). Powders stored at 250°C and 2 % oxygen exhibited the most pronounced effect, showing dark coloring and a mass reduction by 8.9 % after 24 h. This discoloration results from the absorption of wavelength in the visible and UV range of various degradation products produced during thermo-oxidation of PA66 [34]. In contrast, Rolaserit® PA66 aged with lower storage temperature or oxygen content shows reduced yellowing and a lower weight loss of 4.5 %. This is consistent with the findings of Klump [15], who showed that higher temperatures and especially higher oxygen content lead to more pronounced aging effects in PA66. Furthermore, Wiloth et al. [35] reported the release of volatile components at 210 to 220 °C, including hexyl isocyanate and cyclopentylidene-n-hexylamine. These findings may contribute to the weight loss during oven storage. However, further research is needed to validate the nature and extent of molecular changes in PA66 during thermal aging under PBF-LB/P processing conditions. In contrast, the modified powders show less yellowing after processing (Rolaserit® PA66-CP08-CF) and a less pronounced weight loss after 24 hours of oven storage (Rolaserit® PA66-CP08), suggesting improved aging resistance.

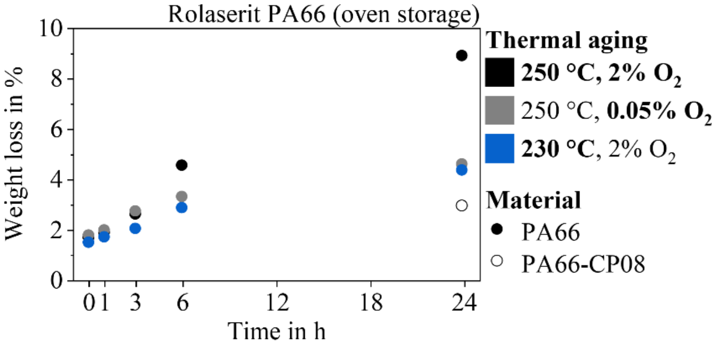

Figure 3: Time-dependent weight loss of Rolaserit® PA66 powder samples during oven storage at different temperatures and oxygen contents

3.2 Influence of thermal ageing on thermal properties

The melting and crystallization behavior of Rolaserit® PA66 undergoes a significant change during oven storage at 250 °C and 2 % oxygen (Fig. 4a). With increasing storage time, the onset and peak of melting and crystallization shift to lower temperatures (Fig. 5a), while the peak height (Fig. 4a) decreases. After 6 h of oven storage, the decrease in the melting temperature is so advanced that the reuse of PA66 powder in subsequent PBF-LB/P processes becomes challenging. This is because a 1:1 blend of virgin and used powder would result in the curling of parts or melting of the powder without laser exposure.

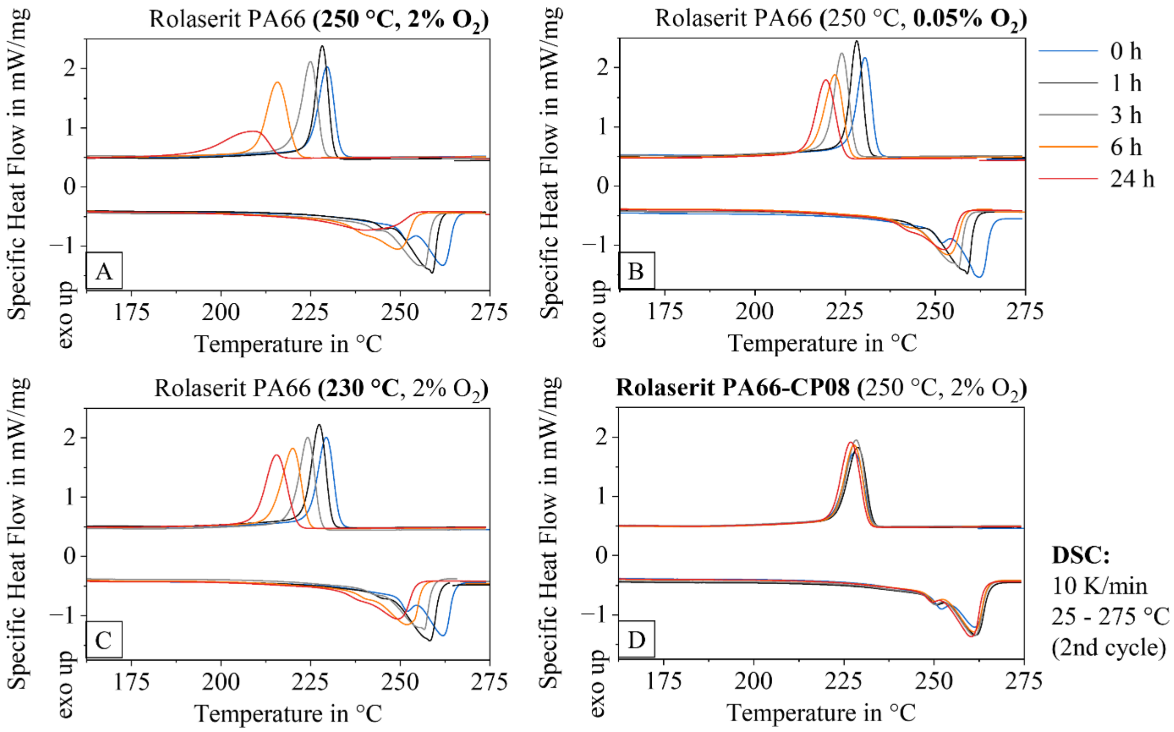

DSC:
10 K/min
25 - 275 °C
(2nd cycle)

Figure 4: Exemplary DSC thermograms for the time-dependent thermal aging of Rolaserit® PA66 at 250 °C after oven storage in a nitrogen atmosphere with 2 % oxygen (A), at 250 °C and 0.05 % oxygen (B), at 230 °C and 2 % oxygen (C), and Rolaserit® PA66-CP08 at 250 °C and 2 % oxygen (D)

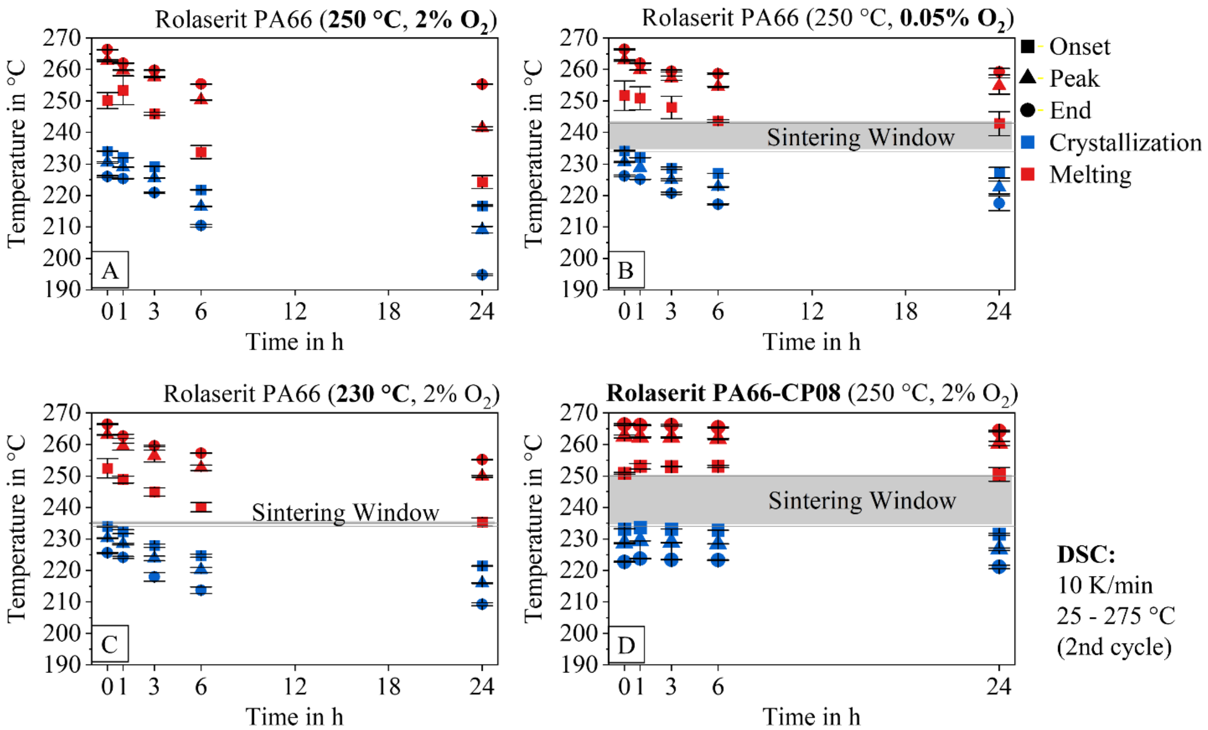

DSC:
10 K/min
25 - 275 °C
(2nd cycle)

Figure 5: Time-dependent thermal aging of the melting and crystallization temperature ranges of Rolaserit® PA66 after oven storage at 250 °C in a nitrogen atmosphere with 2 % oxygen (A), at 250 °C and 0.05 % oxygen (B), at 230 °C and 2 % oxygen (C), and Rolaserit® PA66-CP08 at 250 °C and 2 % oxygen (D)

This change suggests a reduction in the polymer's molecular mass, likely caused by thermo-oxidation (chain scission). Shorter chains in lower molecular weight polymers have greater mobility. This means they can wiggle and rearrange themselves more easily during cooling. This enhanced mobility allows them to pack into a partially ordered, crystalline structure at a higher rate of supercooling than their higher molecular weight counterparts. Similarly, the shorter chains in lower molecular weight polymers require less energy to disrupt the crystal structure during heating. Consequently, the polymer melts at a lower temperature than the one with a higher molecular weight. The broadening of peaks with increasing storage time is likely caused by the presence of degraded, shorter chain fragments alongside some remaining longer chains and byproducts formed during thermo-oxidation, which might have lower melting points than PA66.

A reduction in storage temperature by 20 K (Fig. 4c and 5c) positively influences aging behavior and reduces thermo-oxidative effects. However, the resulting difference between the melting and crystallization temperature of virgin and used powder remains small (233.9–235.3 °C, Δ = 1.4 K), making processing prone to curling. Nevertheless, it can be concluded that a low build chamber temperature is desirable to reduce the aging of PA66 in PBF-LB/P. However, while elevated processing temperatures enhance oxidation, this phenomenon reduces the thickness of an oxidized surface layer [20]. Consequently, future studies should investigate the formation of an oxygen diffusion-limiting layer as a function of particle size and processing conditions, as this can potentially preserve the properties in the particle core.

The samples stored at 0.05 % oxygen (Fig. 4b and 5b) show that the melting and crystallization temperature ranges are less affected by thermo-oxidative effects in low oxygen atmospheres compared to lower chamber temperatures (Fig. 4). This implies that efficient nitrogen purging of the system is a prerequisite for robust processing of PA66 in PBF-LB/P. It should also be noted that, regardless of the oxygen content and storage temperature, after 1 h of oven storage, the width of the crystallization peak decreases while its height increases (Fig. 4), indicating changes in crystallinity. However, further studies are necessary to explain this behavior in more detail as changes in the degree of crystallinity can be attributed to changes in the molecular weight caused by thermo-oxidation [36] as well as to physical aging mechanisms, such as recrystallization.

In contrast, the aging effects are significantly reduced for the modified Rolaserit® PA66-CP08, even at 250°C and 2 % oxygen. Fig. 5 demonstrates that the sintering window for a 1:1 blend of used and virgin powder is relatively broad (233.6 to 250.5 °C, Δ = 16.9 K), as the difference between the onset of melting and the onset of crystallization is nearly identical before and after 24 h oven storage. Consequently, the PA66-CP08 appears to offset the effects that lead to chain scission (thermo-oxidation) and the opposing effects that lead to the extension of molecular chains (post-condensation). This is a prerequisite for robust processing with high rates of used powder. However, further research is required to examine the causes of this behavior.

3.3 Influence of thermal ageing on rheological properties

Examining rheological properties in Fig. 6a confirms the assumption that Rolaserit® PA66 undergoes significant thermo-oxidation during oven storage. In the initial hours of oven storage, the MVR value increases considerably, indicating a decrease in viscosity and, thus, chain scission. However, for prolonged storage periods, the MVR decreases (equivalent to a viscosity increase). This suggests that post-condensation of shorter chains occur following thermo-oxidation [15].

Similarly, the Rolaserit® PA66-CP08 aged at 250 °C and 2 % oxygen shows an increase in MVR initially (Fig. 6b) indicating thermo-oxidative effects. However, the MVR decreases again for more extended storage periods, indicating the presence of post-condensation effects. However, this trend was not observed in the thermal properties since the melt flow index is more sensitive to molecular changes resulting from material aging than a DSC analysis [36].

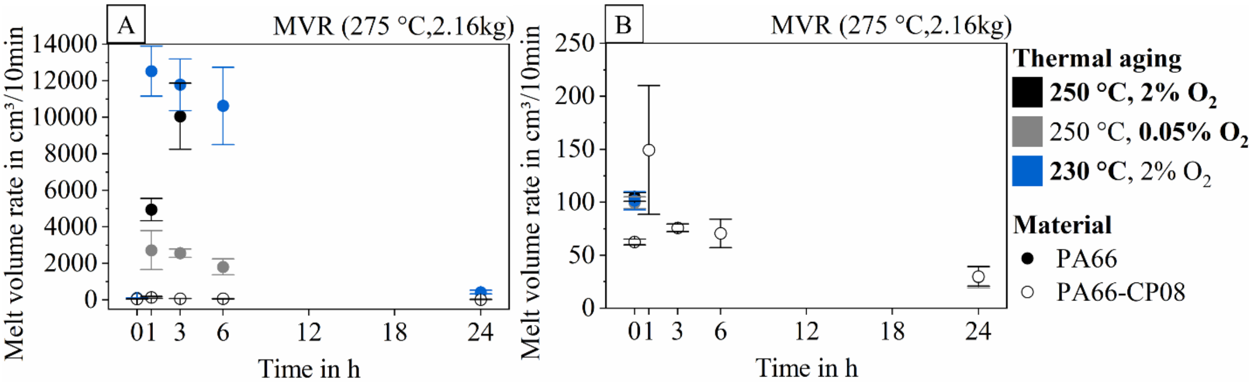

Figure 6: Time-dependent thermal aging of the melt flow rate for Rolaserit® PA66 and PA66-CP08 after oven storage at different temperatures and oxygen contents (A) with an enlarged view for lower melt flow rates (B)

A reduction in storage temperature and, in particular, oxygen content positively affects the reduction of aging behavior in Rolaserit® PA66. Since the polymer powder is dried before oven storage, the influence of hydrolysis caused by residual moisture is considered negligible. However, the Rolaserit® PA66 aged at 0.05 % oxygen still exhibits an increased MVR, which could be partly attributed to chain scission by hydrolysis. Nevertheless, during the thermal aging, the equilibrium shifts to post-condensation. This is exemplified by the MVR of the Rolaserit® PA66 stored at 0.05 % oxygen (29.4 mm³/10 min), which is comparable to that of the modified Rolaserit® PA66-CP08 stored at 2 % oxygen (30.0 mm³/10 min) after 24 h of oven storage. Further research is required to evaluate if the oxidized surface layer reached an equilibrium for these materials and processing conditions.

Lastly, it should be noted that the test conditions for determining the MVR are optimized for the filled PA66 powders to ensure comparability of the results in future studies. For this reason, the MVR values shown in Fig. 6a lie outside the standard's recommended measuring range (< 100 cm³/10min). This reduces the experiment's reproducibility, reflected in the high standard deviations. Moreover, after 6 h of oven storage at 250 °C and 2 % oxygen, MVR experiments reveal inhomogeneous melt extrusion in Rolaserit® PA66 due to decomposed and unmolten particles.

3.4 Influence of laser and scan parameters and powder recycling on part properties

The mechanical properties and density of PA66 are evaluated in the as-built (dry) state. For Rolaserit® PA66-CP08, the tensile strength is relatively unaffected by the process parameters, with values in the xy-direction around 80 MPa (Fig. 7). Similarly, the Young's modulus is around 3100 MPa for all energy densities (Fig. 7). Therefore, the observed discolorations of the powder after processing (Fig. 2) and of the produced tensile test samples do not influence the mechanical properties.

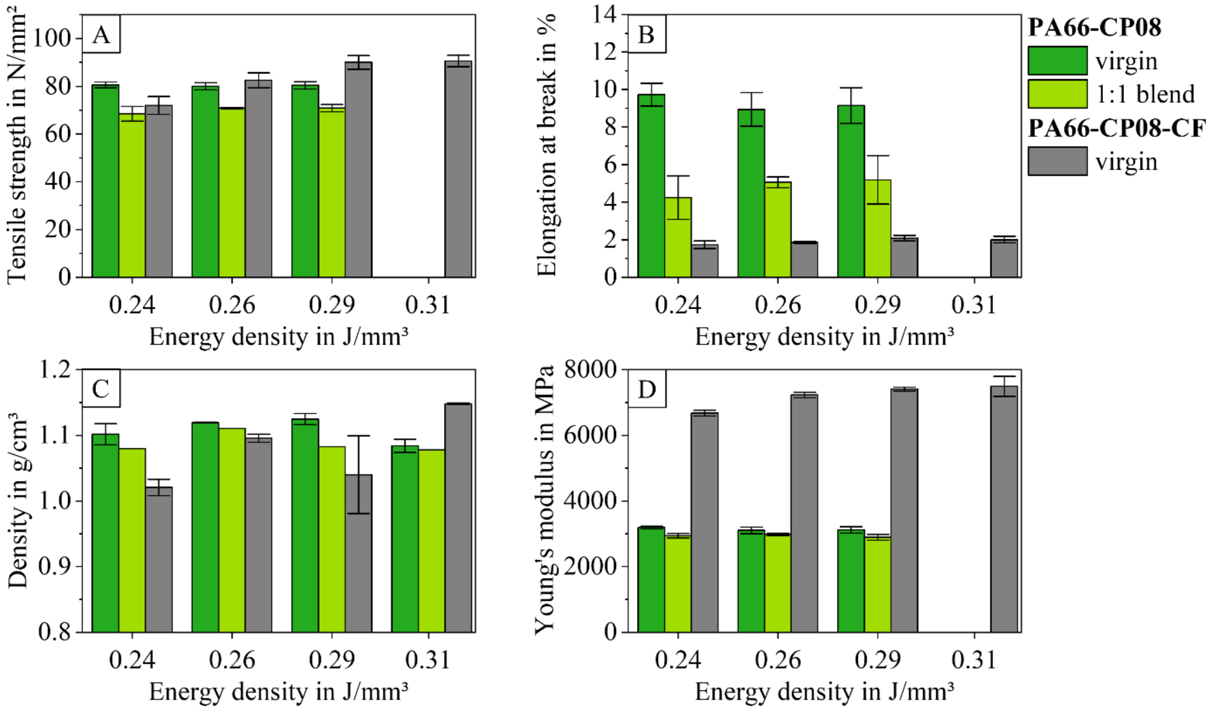

Figure 7: Tensile strength (A), elongation at break (B), density (C), and Young's modulus (D) of samples produced from virgin and recycled (1:1 blend of virgin and used powder) Rolaserit® PA66-CP08 and PA66-CP08-CF

The tensile strength is slightly reduced for a 1:1 blend of virgin and used powder, ranging from 68 to 71 MPa. Similarly, Young's modulus reaches only up to 2980 MPa. While the elongation at break of Rolaserit® PA66-CP08 reaches 9.7 % in the x-direction, the 1:1 blend of used and virgin powder shows less ductility with an elongation of break of only 5.2 % at 0.29 J/mm^3. The density (1.12 g/cm^3 at 0.29 J/mm^3) is slightly below the solid density (1.14 g/cm^3), indicating low porosity. However, density ranges from 1.08 to 1.11 g/cm^3 for 1:1 virgin and used powder blends. The reduced density and mechanical properties are potentially linked to the increased viscosity of the aged Rolaserit® PA66-CP08 (Fig. 6), as reduced melt flowability hinders particle fusion during processing. Since only a limited range of process parameters is evaluated in this work, further research is required to evaluate whether higher energy inputs can improve the mechanical properties and density of 1:1 blends of virgin and used powder.

The Young's modulus of the filled Rolaserit® PA66-CP08-CF is 7500 MPa (at 0.31 J/mm^3) (Fig. 7), which represents a nearly doubling of the stiffness compared to the unfilled Rolaserit® PA66-CP08. Similarly, the filled variant's tensile strength exceeds the unfilled material's values, reaching up to 90.5 MPa (at 0.31 J/mm^3). However, this is accompanied by a considerable reduction in elongation at break (1.7 to 2.1 % in the x-direction), a typical phenomenon for many carbon fiber-filled materials.

The maximum density of Rolaserit® PA66-CP08-CF is achieved at 0.31 J/mm^3, consistent with the mechanical properties. Since the solid density of the filled material is 1.26 g/cm^3, a relative density of around 91 % (1.02 to 1.15 g/cm^3) is achieved for the virgin Rolaserit® PA66-CP08-CF. As shown in Fig. 8, similar tensile strength (85.4 to 88.8 MPa) and density (1.12 to 1.13 g/cm^3) are achieved by the other filled powder variant, Rolaserit® PA66-CP08-CF04.

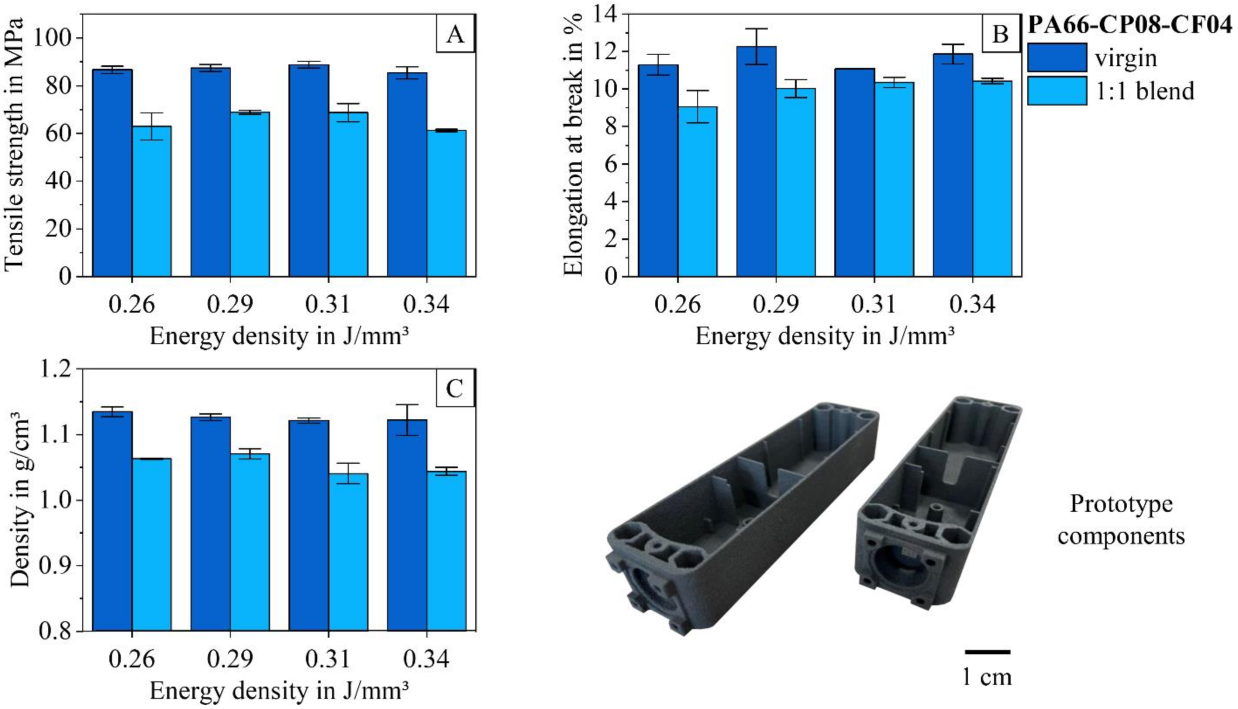

Figure 8: Tensile strength (A), elongation at break (B), and density (C) of PBF-LB/P samples produced from Rolaserit® PA66-CP08-CF04 in virgin and recycled (1:1 blend of virgin and used powder) condition

Furthermore, an elongation at break of 11.1 to 12.3 % is recorded. However, this value is recorded on a different testing machine with no precision extensometer but measuring via the movement of the machine's traverse. Consequently, direct comparison to other development grades of Rolaserit is not possible. Nevertheless, Fig. 8 illustrates that when a 1:1 blend of virgin and used Rolaserit® PA66-CP08-CF04 is processed, there is a decline in mechanical properties, with a 21 % reduction in tensile strength (68.9 MPa at 0.29 J/mm³) and a 12 % decline in elongation at break (10.4 % at 0.29 J/mm³). This is likely attributed to an increase in viscosity resulting from material aging, as indicated by the decrease in density (1.04 to 1.07 g/cm³). However, further research is necessary to determine the cause of the deterioration of the mechanical properties of filled PA66 powders, as the addition of fillers directly influences the material and powder properties. [4]. Moreover, incorporating fillers in PA66 component can enhance the thermo-oxidative stability of mechanical properties yet concurrently diminish the fiber-matrix bonding [20]. However, this is only the case if the filler acts as a barrier limiting oxygen diffusion near the surface. Therefore, the aging behavior of the powder is not affected by the filler in dry-blends.

Fig. 9 shows that the HDT A of Rolaserit® PA66-CP08 is 101 °C (1.8 MPa), while 227 ° C is reached for HDT B (0.45 MPa). Consequently, the unfilled powder can only be used at low mechanical loads at high temperatures without deforming excessively. Conversely, the HDT A and HDT B reach 230 °C and 258 °C, respectively, for the filled Rolaserit® PA66-CP08-CF, thus enabling applications in environments above 200 °C.

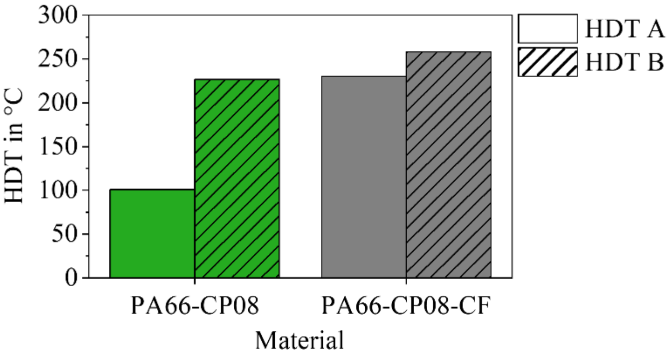

Figure 9: Heat deflection temperature (HDT A and HDT B) of PBF-LB/P samples produced from Rolaserit® PA66-CP08 and PA66-CP08-CF

Conclusion and Outlook

PBF-LB/P exposes polymeric materials to near-melting temperatures for extended periods, causing aging mechanisms that alter the polymer's molecular structure. Consequently, common powder materials such as PA12 require blending with virgin powder to maintain desired properties, while high-performance plastics such as PEEK, processed at high temperatures (>200°C), experience a significant reduction in mechanical properties upon reuse. A cost-effective alternative for aerospace or automobile applications is PA66, which offers lower processing and service temperatures while achieving comparable mechanical properties as a filled compound. However, to date, no PA66 powder material can be processed reliably and reproducibly using PBF-LB/P. This is due to the degradation of the material properties of PA66 when subjected to processing temperatures of approximately 250 °C.

Therefore, this work investigated the influence of aging mechanisms on the material and powder properties of PA66 for the processing conditions in PBF-LB/P. Since neat PA66 cannot be processed directly at this stage, oven storage experiments were performed at first to gain deeper insight into the thermal and rheological properties during thermal storage of neat PA66 and a new modified version of a PA66 powder, called Rolaserit® PA66-CP08. Once a suitable processing temperature range was identified, the printability and material properties of parts made from virgin PA66 powder and a 1:1 blend with used powder were tested. Afterward, the influence of fillers on processability and mechanical properties was also investigated. This research identifies a processing temperature range, laser, and scan parameters at which PA66 powder can be robustly processed and reused. Furthermore, this study determined the mechanical properties that can be achieved with filled and unfilled PA66 in PBF-LB/P. The examined PA66 powders outperformed the market-dominant PA12. Thus, PA66 enables high-temperature applications previously only possible using high-performance polymers such as PEEK. The results of this work can be summarized as follows:

- The particle size of the studied PA66 powders ranges from 15 to 115 µm, resulting in good flowability in virgin and used conditions despite the aged powder exhibiting yellowing.
- The rheological and thermal properties of neat PA66 deteriorate significantly with increased storage time, temperature, and oxygen content. Initially, the MVR of the dried powder increases during oven storage, suggesting the occurrence of strong thermo-oxidation,

followed by post-condensation, as evidenced by a subsequent decrease in MVR for extended storage times.

- In contrast, the melting and crystallization temperatures of the modified Rolaserit® PA66-CP08 indicate a wide sintering window (233.6 to 250.5 °C, Δ = 16.9 K), which enables robust processing for 1:1 blends of used and virgin powder.
- Rolaserit® PA66-CP08 maintains a tensile strength of > 70 MPa and Young's modulus of around 3000 MPa when using 50 % recycled material. Furthermore, an elongation at break of around 9.7 % is reached, although only for virgin powder in the x-direction.
- The filled Rolaserit® PA66-CP08-CF exhibits a Young's modulus > 7000 MPa and a tensile strength of up to 90 MPa in the x-direction. The filled Rolaserit® PA66-CP08-CF04, shows similar values. However, the mechanical properties are slightly reduced when using 50 % recycled material (Tensile strength of 68.9 MPa at 0.26 J/mm^3)
- The filled Rolaserit® PA66-CP08-CF exhibits heat deflection temperatures of 230 °C (HDT A) and 258 °C (HDT B).

In conclusion, the current development grades of Rolaserit® PA66-CP08 and PA66-CP08-CF demonstrate an improved balance of thermo-oxidation and post-condensation for the processing conditions in PBF-LB/P compared to neat PA66. However, further research is required to examine the anisotropy of part properties and the drop in mechanical properties when using 50 % recycled material. Of particular interest is the influence of fillers on aging behavior and the influence of diffusion limitations, which may restrict the oxidation process to a thin layer. In addition, a thermal gravimetric analysis (TGA), coupled with Fourier-transform infrared spectroscopy (FTIR) or mass spectrometry, can provide further insight into the type and ratio of aging mechanisms of PA66 in PBF-LB/P.

Abbreviations

DSC	Differential scanning calorimetry
FTIR	Fourier-transform infrared spectroscopy
HDT	Heat deflection temperature
MVR	Melt volume rate
PA12	Polyamide 12
PA6	Polyamide 6
PA66	Polyamide 66
PE	Polyethylene
PEEK	Polyetheretherketone
PEKK	Polyetherketoneketone
PEAK	Polyaryletherketone
PP	Polypropylene
PPS	Polyphenylene sulfide
TGA	Thermal gravimetric analysis
TPU	Thermoplastic polyurethane

Acknowledgements

The project "CyclePA66 - Increasing the recycling rates of filled PA66 powder materials for laser sintering" on which this report is based, was funded by the German Federal Ministry of Education and Research (Bundesministeriums für Bildung und Forschung, BMBF) under the grant number 03XP0546C. The authors are responsible for the content of this publication.

References

1. Wudy K, Drummer D (2019) Aging effects of polyamide 12 in selective laser sintering: Molecular weight distribution and thermal properties. Additive Manufacturing 25:1–9. https://doi.org/10.1016/j.addma.2018.11.007
2. Dotchev K, Yusoff W (2009) Recycling of polyamide 12 based powders in the laser sintering process. Rapid Prototyping Journal 15:192–203. https://doi.org/10.1108/13552540910960299
3. Yang F, Schnuerch A, Chen X (2021) Quantitative influences of successive reuse on thermal decomposition, molecular evolution, and elemental composition of polyamide 12 residues in selective laser sintering. Int J Adv Manuf Technol 115:3121–3138. https://doi.org/10.1007/s00170-021-07368-w
4. Kusoglu IM, Doñate-Buendía C, Barcikowski S et al. (2021) Laser Powder Bed Fusion of Polymers: Quantitative Research Direction Indices. Materials (Basel) 14. https://doi.org/10.3390/ma14051169
5. Ghita OR, James E, Trimble R et al. (2014) Physico-chemical behaviour of Poly (Ether Ketone) (PEK) in High Temperature Laser Sintering (HT-LS). Journal of Materials Processing Technology 214:969–978. https://doi.org/10.1016/j.jmatprotec.2013.11.007
6. AM-Rauch GmbH & CoKG (2019) Datasheet PPS – GF25 (Polyphenylene Sulfide Glas Reinforced – Toraymill® PPS – GF 25)
7. Xue C, Chu M, Yang Y et al. (2021) A Study on the Analysis and Prediction of the Anisotropy of Injection Molded GF/PA66. J Phys.: Conf Ser 1790:12055. https://doi.org/10.1088/1742-6596/1790/1/012055
8. Ehrenstein GW, Pongratz S (2013) Resistance and stability of polymers. Hanser, München
9. Wudy K, Drummer D, Kühnlein F et al. (2014) Influence of degradation behavior of polyamide 12 powders in laser sintering process on produced parts. In: American Institute of Physics, pp 691–695
10. El-Mazry C, Ben Hassine M, Correc O et al. (2013) Thermal oxidation kinetics of additive free polyamide 6-6. Polymer Degradation and Stability 98:22–36. https://doi.org/10.1016/j.polymdegradstab.2012.11.002
11. White G von, Smith JN, Clough RL et al. (2012) The origins of CO2 and NH3 in the thermal-oxidative degradation of nylon 6.6. Polymer Degradation and Stability 97:1396–1404. https://doi.org/10.1016/j.polymdegradstab.2012.05.018
12. White G von, Clough RL, Hochrein JM et al. (2013) Application of isotopic labeling, and gas chromatography mass spectrometry, to understanding degradation products and pathways in the thermal-oxidative aging of Nylon 6.6. Polymer Degradation and Stability 98:2452–2465. https://doi.org/10.1016/j.polymdegradstab.2013.08.029
13. Allen NS, Harrison MJ, Follows GW et al. (1987) Thermal and photo-chemical degradation of nylon 6,6 polymer: Part 1—Influence of amine-carboxyl end group balance on

luminescent species. Polymer Degradation and Stability 19:77–95. https://doi.org/10.1016/0141-3910(87)90014-0

14. Eriksson P-A, Boydell P, Eriksson K et al. (1997) Effect of thermal-oxidative aging on mechanical, chemical, and thermal properties of recycled polyamide 66. J Appl Polym Sci 65:1619–1630. https://doi.org/10.1002/(SICI)1097-4628(19970822)65:8<1619:AID-APP18>3.0.CO;2-Q
15. Klump K (2021) Stabilisation of polyamides during long-term storage at high temperatures, Technical University of Darmstadt, Chemistry Department
16. SZWARC M (1956) 'Living' Polymers. Nature 178:1168–1169. https://doi.org/10.1038/1781168a0
17. Papaspyrides CD, Vouyiouka SN (2009) Solid State Polymerization. Wiley
18. Audouin L, Langlois V, Verdu J et al. (1994) Role of oxygen diffusion in polymer ageing: kinetic and mechanical aspects. Journal of Materials Science 29:569–583. https://doi.org/10.1007/BF00445968
19. Celina MC (2013) Review of polymer oxidation and its relationship with materials performance and lifetime prediction. Polymer Degradation and Stability 98:2419–2429. https://doi.org/10.1016/j.polymdegradstab.2013.06.024
20. Sang L, Wang C, Wang Y et al. (2017) Thermo-oxidative ageing effect on mechanical properties and morphology of short fibre reinforced polyamide composites – comparison of carbon and glass fibres. RSC Adv 7:43334–43344. https://doi.org/10.1039/c7ra07884f
21. Gijsman P, Dong W, Quintana A et al. (2016) Influence of temperature and stabilization on oxygen diffusion limited oxidation profiles of polyamide 6. Polymer Degradation and Stability 130:83–96. https://doi.org/10.1016/j.polymdegradstab.2016.05.024
22. Ahlblad G, Forsström D, Stenberg B et al. (1997) Oxidation profiles of polyamide 6,6 studied by imaging chemiluminescence and FTIR. Polymer Degradation and Stability 55:287–293. https://doi.org/10.1016/S0141-3910(96)00164-4
23. Puffr R, Šebenda J (1967) On the Structure and Properties of Polyamides. XXVII. The Mechanism of Water Sorption in Polyamides. J polym sci., C Polym symp 16:79–93. https://doi.org/10.1002/polc.5070160109
24. Reuvers NJW, Huinink HP, Fischer HR et al. (2012) Quantitative Water Uptake Study in Thin Nylon-6 Films with NMR Imaging. Macromolecules 45:1937–1945. https://doi.org/10.1021/ma202719x
25. Broudin M, Le Gac PY, Le Saux V et al. (2015) Water diffusivity in PA66: Experimental characterization and modeling based on free volume theory. European Polymer Journal 67:326–334. https://doi.org/10.1016/j.eurpolymj.2015.04.015
26. Chaupart N, Serpe G, Verdu J (1998) Molecular weight distribution and mass changes during polyamide hydrolysis. Polymer 39:1375–1380. https://doi.org/10.1016/S0032-3861(97)00414-X
27. Jacques B, Werth M, Merdas I et al. (2002) Hydrolytic ageing of polyamide 11. 1. Hydrolysis kinetics in water. Polymer 43:6439–6447. https://doi.org/10.1016/S0032-3861(02)00583-9
28. Hernandez RJ (1994) Effect of water vapor on the transport properties of oxygen through polyamide packaging materials. Journal of Food Engineering 22:495–507. https://doi.org/10.1016/0260-8774(94)90050-7
29. Valko EI, Chiklis CK (1965) Effects of thermal exposure on the physicochemical properties of polyamides. J Appl Polym Sci 9:2855–2877. https://doi.org/10.1002/app.1965.070090820

30. Schaffer MA, McAuley KB, Marchildon EK et al. (2007) Thermal Degradation Kinetics of Nylon 66: Experimental Study and Comparison with Model Predictions. Macro Reaction Engineering 1:563–577. https://doi.org/10.1002/mren.200700020
31. Hofmann J, Wudy K (2022) In situ process monitoring in laser-based powder bed fusion of polyamide 12 using thermal imaging. Int J Adv Manuf Technol 122:4127–4138. https://doi.org/10.1007/s00170-022-10169-4
32. Schmid M, Amado A, Wegener K (2015) Polymer powders for selective laser sintering (SLS). In: AIP Publishing LLC, p 160009
33. Guo X, Moudgil BM (2024) Role of Powder Properties and Flowability in Polymer Selective Laser Sintering—A Review. KONA 41:26–41. https://doi.org/10.14356/kona.2024012
34. Karstens T, Rossbach V (1989) Thermo-oxidative degradation of polyamide 6 and 6,6. Kinetics of the formation and inhibition of UV/VIS-active chromophores. Makromol Chem 190:3033–3053. https://doi.org/10.1002/macp.1989.021901201
35. Wiloth F, Schindler E (1970) Zur thermischen Zersetzung von Nylon 66, II. Thermolyse von 2-[n-Hexylimino]-cyclopentan-carbonsäure-(1)-n-hexylamid Isocyanatabspaltung aus α-Carbamoyl-cyclopentanoniminen. Chem Ber 103:757–765. https://doi.org/10.1002/cber.19701030315
36. Pham DT, Dotchev KD, Yusoff WAY (2008) Deterioration of polyamide powder properties in the laser sintering process. Proceedings of the Institution of Mechanical Engineers, Part C: Journal of Mechanical Engineering Science 222:2163–2176. https://doi.org/10.1243/09544062JMES839